6

Intravoxel incoherent motion analysis of the liver of Fontan patients

H. Dijkstra, D. Wolff, J.P. van Melle, B. Bartelds, T.P. Willems, H. Hillege, A.P. van den Berg, T. Ebels, R.M.F. Berger, P.E. Sijens

Abstract

Background: Mean hepatic apparent diffusion coefficients (ADC) decreases in patients with a Fontan circulation. It remains unclear whether this is a true decrease of molecular diffusion, or rather reflects decreased microperfusion due to decreased portal blood flow.

Methods: This study was aimed to use Intravoxel incoherent motion analyses modeled diffusion-weighted imaging (IVIM-DWI) (using 9 b-values) to differentiate diffusion and microperfusion for eight liver segments in 59 patients with a Fontan circulation, compare the results with a control group, and further explore the relationship with parameters associated with functional status, chronic congestion and hepatic disease.

Results: Microperfusion parameters (D_{fast} and f_{fast}) were reduced ($p < 0.001$) in Fontan patients compared to healthy volunteers with −38.1% for D_{fast} and −32.6% for f_{fast}. Molecular diffusion (D_{slow}) was similar in patients and healthy volunteers, while the ADC was significantly lower (−14.3%) in patients ($p < 0.001$). The ADC showed a significant negative linear relationship with the follow-up duration after Fontan operation with a correlation coefficient $r=-0.657$, with the highest correlations found in segments II and VIII. Molecular diffusion also showed significant negative linear relationship ($r=-0.591$) with follow-up duration whereas the microperfusion parameters did not.

Conclusions: Decreased hepatic ADC in Fontan patients reflects lowered microperfusion of the Fontan liver rather than decreased diffusion. The ADC values and molecular diffusion decreased with the follow-up duration after Fontan operation, whereas the microperfusion was stable over time. The current study is the first to show with IVIM-DWI that, in a Fontan circulation, the development of liver fibrosis-/cirrhosis varies between the different liver segments, depending on the degree of arterial blood supply.

Introduction

Diffusion-weighted imaging (DWI) has been successfully applied in the assessment of diffuse liver diseases such as cirrhosis, fibrosis and steatosis[1-7]. Cirrhotic livers had significantly lower apparent diffusion coefficients (ADC) than normal livers[1,4,5] and negative correlations between fibroses stages and ADC values were demonstrated[3,6-8]. The ADC is obtained by calculating a mono-exponential fit from multiple (al least two) diffusion-weighted images, thereby integrating molecular diffusion and microperfusion effects in one quantitative parameter[9,10]. The concept of the ADC however has been derived from the more complex intravoxel incoherent motion (IVIM) model, which separates molecular diffusion and microperfusion effects by fitting a bi-exponential model to multiple DW images[10]. It has been suggested that the ADC reduction observed in cirrhotic livers could be linked to decreased microperfusion values and may be related to reduced perfusion[4]. A category of patients with altered hepatic perfusion are patients with a Fontan circulation.

Fontan et al. described a palliative operation in which the right atrium (and in newer techniques the caval veins) is directly connected to the pulmonary arteries[11,12]. Additional detail about the Fontan operation is provided in Appendix 1. In the absence of a subpulmonary ventricle, this operation induces increased central venous pressure, decreased preload and increased afterload of the ventricle[13]. In the Netherlands, yearly around 50 newborns born with a complex congenital heart disease, known as the univentricular heart, are treated with this technique[14,15]. Over four decades, the short term survival after the Fontan operation improved significantly, resulting in an increasing cohort of Fontan patients who reach adolescence and adulthood[16]. Consequently, long-term complicatin of the Fontan circulation are more commonly seen. One of the implications of the Fontan circulation is liver disease resulting in fibrosis and cirrhosis[17-20]. A significant positive correlation has been found between the duration (from the day of the Fontan operation) and the degree of hepatic fibrosis[21]. This hepatic damage in the context of a Fontan circulation is presumably caused by the elevated venous pressure and limited cardiac output that causes decreased portal flow[14]. The hepatic artery compensates the diminished portal flow by increased hepatic arterial flow, which is termed the hepatic arterial buffer response (HABR). The distribution of the microperfusion is likely to vary among the different liver segments due to the alternative distribution of the hepatic flow in Fontan patients. In a recent report we showed that mean hepatic ADC are decreased in Fontan patients[22]. It remained unclear whether this is a true decrease of molecular diffusion, or rather reflects decreased microperfusion due to decreased portal blood flow. Therefore, the aim of our current thorough analysis of the same data is to use IVIM modeled DWI to differentiate diffusion and microperfusion for eight liver segments in patients with a Fontan circulation, compare the results with a control group, and further explore the relationship with parameters associated with functional status, chronic congestion and hepatic disease.

Methods

Study population

The protocol of the study was approved by the hospital's institutional review board and informed consent was obtained from each patient. Between January 2012 and October 2013, consecutive patients with a functionally univentricular heart treated with a Fontan operation (further referred to as Fontan patients) were scheduled for MRI and diffusion-weighted imaging (DWI)[22]. Inclusion criteria were: age 10 years or older. This resulted in 59 patients, 32 children and 27 adults (mean age, 19.1 years). Clinical variables included body mass index (BMI), cardiac index, ejection fraction, end-diastolic volume (EDV), laboratory measurements (AST, ALT, gammaGT, FactorVIII, ASTALTratio, bilirubine, albumine, PT, MELDXI, Fib4) and vena cava inferior (VCI) diameter and were obtained using previously described standardized methods[22].

In addition, a control group of volunteers was included in this study: 10 men and 9 women (n=19) ranging from 20 to 62 years old (mean age, 32.9 years)[23]. All subjects were healthy volunteers, without relevant medical history.

MR protocol

Diffusion-weighted imaging (DWI) of the liver was acquired by Magnetic Resonance Imaging (MRI), using a commercially available 1.5 T scanner (Magnetom Aera, Siemens Medical Solutions, Erlangen, Germany). A 32 element spine matrix coil in combination with a 4 element body matrix was used as the receiver, and the body coil as transmitter. The protocol included a routine localizer where after 9 series (b=0, 50, 100, 250, 500, 750, 1000, 1500, 1750 s/mm^2) of DWI were acquired using a spin echo based echo-planar imaging (EPI) sequence using the following parameters: TR 5900-9600 ms; TE 90 ms; slice-thickness 5 mm; slice gap 10 mm; FOV 242×300 mm^2; matrix 116×144; bandwidth 1335 Hz/pixel; averages 4 and parallel acquisition technique GRAPPA with acceleration factor 2. PACE respiratory triggering was enabled and spectral adiabatic inversion recovery (SPAIR) was used for fat suppression to avoid artifacts from subcutaneous fat. In total, between 14 and 16 transverse slices were acquired to cover the whole liver. Circular regions-of-interest (ROIs) of 21.5 mm^2 were drawn in 8 different segments of the liver (segment II, III, IVa, IVb, V, VI, VII, VIII) according to the Couinaud-Bismuth classification[24,25]. Extra care was taken to avoid major blood vessels in the ROIs.

DWI analysis

The control group was acquired using 7 b-values (b = 0, 50, 100, 250, 500, 750, 1000 s/mm^2); therefore only these 7 b-values were used in the comparison between Fontan patients

and controls, whereas the remaining acquired DWI series (b = 1500 and 1750 s/mm^2) were included in all other analyses. The analysis was performed off-line using monoexponential (ADC) and biexponential fitting procedures in a programmable graphical and calculus environment (Matlab, The Mathworks, Natick, MA, USA). In the biexponential analyses, the diffusion-weighted signal intensities S were fitted using the parameters prescribed by the IVIM model[10,26]: $S/S_0 = f_{fast} \cdot \exp(-b \cdot D_{fast}) + f_{slow} \cdot \exp(-b \cdot D_{slow})$ where S_0 is the maximum signal intensity, D_{fast} is the fast component representing microperfusion, f_{fast} is the fraction of microperfusion, D_{slow} is the slow component representing molecular diffusion and f_{slow} is the fraction of molecular diffusion ($f_{slow} = 1 - f_{fast}$). Equation 1 was fitted by the Nelder-Mead simplex direct search method with bound constraints, which performs a constrained non-linear minimization of the sum of the squared residuals[27,28]. The initial guess D^0_{slow} was estimated by calculating the slope of the asymptote of the slow signal component between b = 500 and 1000 s/mm^2, and D_{slow} was bound between 0.2 and $5 \times D^0_{slow} \times 10^{-3}$ mm^2/s. The intercept of the asymptote with the y-axis at S_0 resulted in an initial guess f^0_{fast}, and f_{fast} was bound between 0 and 1. The slope of the signal between b = 0 and b = 50 s/mm^2 was used to guess the initial value of the fast signal component (D^0_{fast}), and D_{fast} was bound between D^0_{slow} (microperfusion can never be slower than molecular diffusion) and 100×10^{-3} mm^2/s. The ADC was obtained by using a clinically accepted method: a mono-exponential fit of all b-values was performed.

Statistics

Statistical analyses were performed using SPSS (SPSS 20, Chicago, IL, USA). All data were tested for normality using Shapiro–Wilk tests. Measurements were assessed per segment and also averaged over all segments. Normally distributed data (ADC, D_{slow}, D_{fast}, f_{fast}, AST, ALT, gammaGT, FactorVIII, AST ALTratio, EDV, EF, Cardiac index) were shown as means with standard deviations. Non-normally distributed data (BMI, Bilirubine, Albumine, PT, MELD XI, Fib4, Vena cava inferior – VCI diameter and follow-up duration) were shown as medians with interquartile range.

Differences of DWI data between patients and volunteers were compared by independent samples t-tests. Differences among the segments were tested using one-way ANOVA tests.

Correlations were calculated using a linear ($Y = a \cdot X + b$) model using Pearson's correlation coefficient for normally distributed variables and Spearman's rank correlation coefficient for non-normally distributed variables.

Results

IVIM-DWI parameters and ADC were normally distributed ($p \geq 0.071$). Microperfusion parameters (D_{fast} and f_{fast}) averaged over all segments were significantly ($p < 0.001$) lower in Fontan patients compared to healthy volunteers with −38.1% for D_{fast} and −32.6% for f_{fast} (Table 1). Molecular diffusion (D_{slow}) was similar in patients and healthy volunteers, while the ADC was significantly lower (−14.3%) in patients ($p < 0.001$).

Table 1. Data averaged over all segment and shown as mean ± standard deviations

	Patients	Volunteers	P
ADC ($\times 10^{-3}$ mm^2/s)	1.08 ± 0.11	1.26 ± 0.11	<0.001*
D_{slow} ($\times 10^{-3}$ mm^2/s)	0.95 ± 0.14	1.00 ± 0.13	0.171
D_{fast} ($\times 10^{-3}$ mm^2/s)	23.2 ± 5.8	37.5 ± 7.3	<0.001*
F_{fast}	23.6 ± 4.7	35.0 ± 6.0	<0.001*

Differences of DWI data between patients and volunteers were assessed by independent samples. t-tests. *P-value indicates significant difference.

Also on a segmental level, the microperfusion parameters were significantly decreased for the majority of liver segments of Fontan patients compared to healthy volunteers (Table 2). The molecular diffusion was lower in half of the segments (III, IVb, VI and VII) compared to healthy volunteers (Table 3). The ADC was lower in almost all segments (except segment V).

Concerning the homogeneity of IVIM values among the segments, it was observed that for Fontan patients the microperfusion parameters differed significantly throughout the liver ($p \leq 0.045$). This was also true for the ADC ($p < 0.001$). The molecular diffusion however was similar among the segments ($p=0.208$).

The DWI data averaged over all segments were correlated to the clinical laboratory measurements (Table 4). The ADC showed a significant negative linear relationship with the follow-up duration after Fontan operation with a correlation coefficient $r=-0.657$ (Figure 1), with the highest correlations found in segments II and VIII (Table 5). Also the molecular diffusion showed a significant negative linear relationship ($r=-0.591$) with the follow-up duration, with the highest correlations found in segments V and VIII.

Table 2. Microperfusion data (using 7 b-values) per segment and shown as mean ± standard deviations

	D_{fast} ($\times 10^{-3}$ mm^2/s)				F_{fast} (%)			
Seg.	**Patient**	**Volunteer**	**Δ%**	**P**	**Patient**	**Volunteer**	**Δ%**	**P**
II	27.0 ± 14.1	21.5 ± 8.8	+25.6	0.051	32.6 ± 12.2	58.6 ± 12.1	-79.8	<0.001*
III	24.6 ± 8.9	37.7 ± 22.2	-53.3	0.021*	24.9 ± 9.8	37.9 ± 11.0	-52.2	<0.001*
IVa	23.8 ± 9.5	31.2 ± 17.9	-30.5	0.095	25.1 ± 10.4	39.4 ± 16.9	-57.0	0.002*
IVb	22.9 ± 8.8	46.3 ± 16.9	-202	<0.001*	21.2 ± 7.9	35.1 ± 9.5	-65.6	<0.001*
V	22.2 ± 8.0	37.5 ± 13.2	-68.9	<0.001*	20.4 ± 8.3	29.3 ± 6.9	-43.6	<0.001*
VI	22.4 ± 8.1	45.1 ± 23.7	-201	0.001*	21.3 ± 7.9	27.6 ± 9.2	-29.6	0.012*
VII	21.4 ± 8.9	42.9 ± 25.1	-200	0.002*	21.7 ±6.4	27.1 ± 7.1	-24.9	0.007*
VIII	22.0 ± 8.6	37.8 ± 15.2	-71.8	<0.001*	22.2 ± 7.0	24.9 ± 9.7	-12.2	0.293
P	0.045*	0.001*			<0.001*	<0.001*		

Differences among the segments were tested using one-way ANOVA tests. Differences of DWI data between patients and volunteers were assessed by independent t-tests. *P-value indicates significant difference.

Table 3. Diffusion data (using 7 b-values) per segment and shown as mean ± standard deviations

Segment	ADC ($\times 10^{-3}$ mm^2/s)			D_{slow} ($\times 10^{-3}$ mm^2/s)		
	Patients	**Volunteers**	**P**	**Patients**	**Volunteers**	**P**
II	1.15 ± 0.28	1.42 ± 0.29	<0.001*	0.95 ± 0.36	0.79 ± 0.40	0.123
III	1.10 ± 0.15	1.38 ± 0.15	<0.001*	0.96 ± 0.19	1.12 ± 0.21	0.009*
IVa	1.12 ± 0.16	1.40 ± 0.24	<0.001*	0.97 ± 0.23	1.05 ± 0.38	0.422
IVb	1.09 ± 0.11	1.32 ± 0.15	<0.001*	0.98 ± 0.14	1.12 ± 0.14	0.001*
V	1.05 ± 0.12	1.09 ± 0.18	0.391	0.96 ± 0.17	0.92 ± 0.21	0.482
VI	1.06 ± 0.15	1.18 ± 0.08	<0.001*	0.95 ± 0.17	1.02 ± 0.09	0.021*
VII	1.06 ± 0.14	1.21 ± 0.10	<0.001*	0.93 ± 0.18	1.05 ± 0.13	0.005*
VIII	1.00 ± 0.15	1.09 ± 0.16	0.024*	0.88 ± 0.20	0.94 ± 0.21	0.213
P	<0.001*	<0.001*		0.208	0.001*	

Differences among the segments were tested using one-way ANOVA tests. Differences of DWI data between patients and volunteers were assessed by independent samples t-tests. *P-value indicates significant difference.

The fraction of microperfusion on the other hand showed a significant positive linear relationship (r = +0.361) with the follow-up duration (Figure 2), with the highest correlations in segments V and VIII.

The FIB-4 score showed weak though significant relationships, negative with molecular diffusion (r = −0.322) and positive with the fraction of microperfusion (r = +0.324). Some other clinical laboratory parameters also showed significant correlations with IVIM-DWI parameters, most notably gamma GT with ADC and D_{slow} (r = −0.450 and r = −0.424, respectively; Table 4.

Table 4. Correlations between DWI parameters (using all 9 b-values) and clinical variables were calculated using a linear (Y = a·X + b) model

	ADC	D_{slow}	D_{fast}	F_{fast}
Laboratory				
measurements				
AST†	+0.199	+0.275*	+0.250	-0.132
ALT†	-0.173	-0.188	+0.045	+0.218
gamma GT†	-0.450**	-0.424**	-0.047	+0.199
Bilirubine‡	-0.258	-0.275	+0.198	+0.301*
Albumine‡	+0.127	+0.100	+0.238	+0.110
PT‡	-0.143	-0.180	-0.321*	-0.033
Factor VIII†	+0.046	-0.003	-0.058	+0.005
Liver disease scores				
MELDXI‡	-0.259	-0.271	+0.266	+0.402**
AST-ALT ratio†	+0.330*	+0.405*	+0.203	-0.317*
Fib4‡	-0.344*	-0.322*	-0.020	+0.324*
Cardiac function				
EDV†	+0.153	+0.093	+0.031	+0.131
EF†	+0.043	+0.076	+0.070	-0.106
Cardiac-index†	+0.270*	+0.266*	+0.220	+0.005
VCI diameter ‡	-0.222	-0.211	0.034	0.180
Follow-up duration ‡	-0.657**	-0.591**	-0.158	+0.401**

†Pearson's correlation coefficient. ‡Spearman's rank correlation coefficient. *P-value indicates significant difference on the 5% level. ***P-value indicates significant difference on the 1% level.

Figure 1. Correlation between follow-up time and ADC

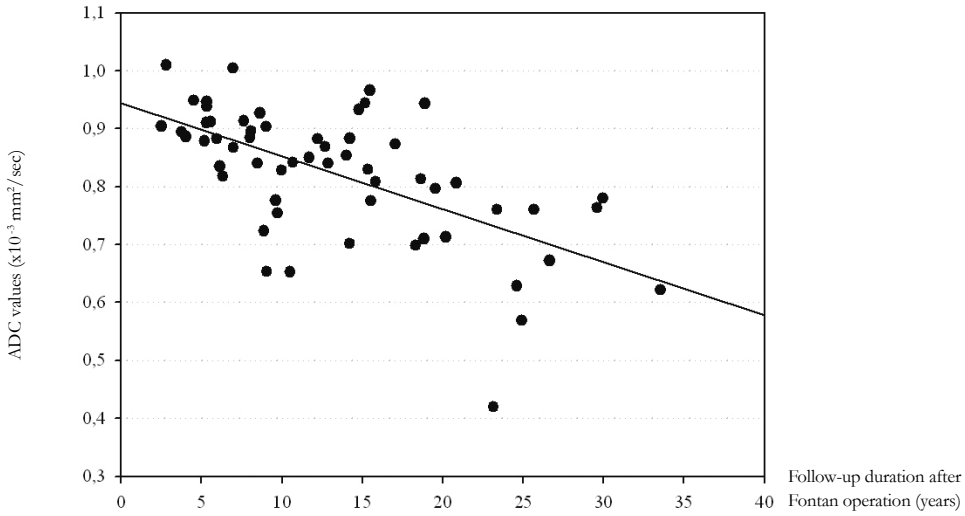

ADC=apparent diffusion coefficents.

Table 5. Correlations per segment between DWI parameters (using all 9 b-values) and follow-up duration were calculated using a linear (Y = a·X + b) model

Segment	ADC	D_{slow}	D_{fast}	F_{fast}
II	-0.632**	-0.307*	+0.002	-0.167
III	-0.447**	-0.397**	+0.067	+0.239
IVa	-0.555**	-0.453**	-0.216	+0.212
IVb	-0.367**	-0.258	+0.013	+0.221
V	-0.562**	-0.556**	-0.120	+0.440**
VI	-0.494**	-0.488**	-0.123	+0.269*
VII	-0.328*	-0.367**	-0.207	+0.203
VIII	-0.612**	-0.567**	-0.154	+0.371**

†Pearson's correlation coefficient. ‡Spearman's rank correlation coefficient. *P-value indicates significant difference on the 5% level. ***P-value indicates significant difference on the 1% level.

Figure 2. Correlation between follow-up time and molecular diffusion (top) and fraction of microperfusion (bottom)

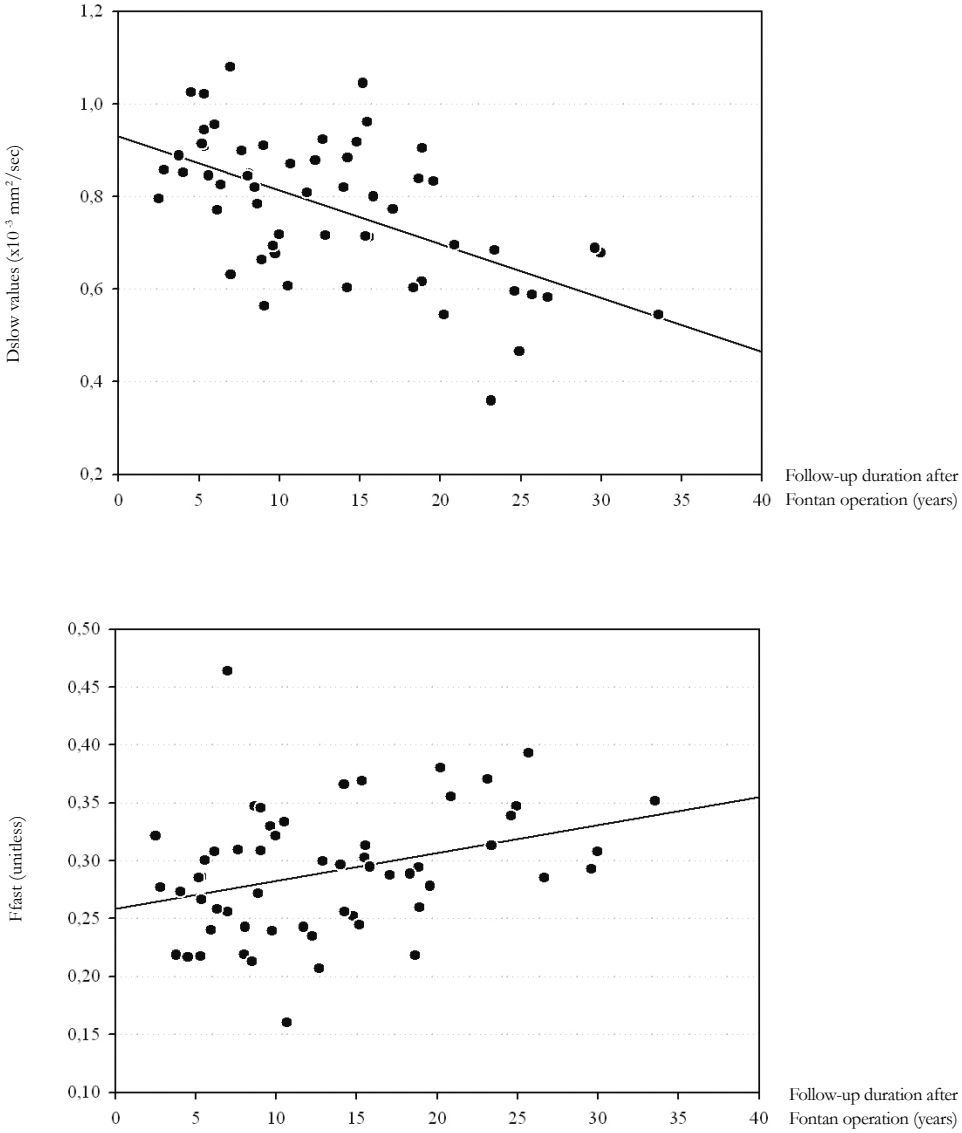

Dslow=cellular diffusion component; Ffast=fraction of microperfusion.

Discussion

In this study it was demonstrated that decreased hepatic ADC measurements of Fontan patients can be explained by significantly lower microperfusion in the Fontan liver rather than by decreased diffusion. It was observed that the molecular diffusion was similar between Fontan patients and healthy volunteers, while the microperfusion parameters (D_{fast} and f_{fast}) and ADC were significantly lower in the Fontan liver. A previously formulated hypothesis relating hypoperfusion of the liver to the reduced ADC in Fontan patients is thus substantiated[22]. However, the here and previously[22] reported strong negative dependency of the liver ADC on the follow-up duration after the Fontan operation rather reflects changes with time in the molecular diffusion than in the microperfusion parameters. This indicates that in the Fontan patient's follow-up true cellular changes leading to fibrosis and cirrhosis dominate over changes in microperfusion.

The evidence in the current study that hypoperfusion of the liver in Fontan patients causes the reduced ADC values as compared with controls, confirms the high degree of sensitivity to microperfusion of the mono-exponential model which was already shown decades ago by Le Bihan et al. in DWI of the brain[10]. When the DWI sequence contains b-values in the microperfusion range ($b \leq 100$ s/mm^2), and the microperfusion is diminished, the ADC measurements will decrease[23]. With a bi-exponential IVIM model, the cellular diffusion component can be distinguished from the microperfusion component, in order to improve our understanding of the underlying pathophysiology of liver disease in the Fontan circulation, and to provide important additional information on the degree of congestion and liver fibrosis-/cirrhosis in clinical practice.

It was observed that the ADC values and molecular diffusion decreased with the follow-up duration after Fontan operation, whereas the microperfusion was stable over time. In other words, the hepatic congestion is chronically present and stable over time, whereas structural liver disease (i.e. liverfibrosis-/cirrhosis) seems not present at first but develops progressively in time after Fontan operation.

All patients had some derangement of laboratory liver measurements; potentially laboratory disturbance is not only associated with advanced liver disease, but also influenced by chronic liver damage, due to congestion and hypoperfusion. Increased gamma GT, a sign of congestive hepatopathy, was rather related to D_{slow} than to the microperfusion. This confirms that D_{slow} is indeed related to liver fibrosis and cirrhosis, and suggests that in the liver these processes might develop faster in context of more liver congestion (as in the first case report by Lemmer in 1983)[29].

Previous histological studies have demonstrated, on a microscopic level, that in patients with chronic hepatic congestion, the poorly arterially supplied hepatocytes in the centrilobular zone show atrophy[30,31]. In patients with a Fontan circulation, atrophy of centrilobular hepatocytes seems related to the degree of right sided pressure and to the time after Fontan

operation[21,31]. Likewise, on a macroscopic level, the arterial blood supply is not homogenously distributed over the various liver segments. It has been reported that the ratio of the arterial liver perfusion (ALP) and portal venous perfusion (PVP) varies and is the lowest in segments V to VIII and highest in segments I to IV[32,33]. When the ALP over-compensates the PVP in Fontan patients, it is expected that the microperfusion increases in segments I to IV, and diminishes in segments V to VIII. This is confirmed by our data. We believe that the current study is the first to show that, in a Fontan circulation, the development of liver fibrosis-/cirrhosis varies between the different liver segments, depending on the degree of arterial blood supply.

Conclusions

Decreased hepatic ADC measurements of Fontan patients can be explained by significantly lower microperfusion of the Fontan liver, instead of a decreased diffusion. It was observed that the ADC values and molecular diffusion decreased with the follow-up duration since the Fontan operation, whereas the microperfusion was stable over time. We believe that the current study is the first to show with IVIM-DWI that, in a Fontan circulation, the development of liver fibrosis-/cirrhosis varies between the different liver segments, depending on the degree of arterial blood supply.

Al together, this study demonstrated that the degree of congestion is generally stable with time after Fontan operation, but liver fibrosis/-cirrhosis develops progressively. With the bi-exponential model, the DWI-MR technique provides the opportunity to distinguish between these two components. For clinical practice, this provides a major advantage compared to the other non-invasive alternatives for liver biopsy. Potentially, a decrease in the microperfusion component could indicate an adverse change in the Fontan circulation, for instance more congestion due to a conduit stenosis or pulmonary vascular remodeling. With a routine follow-up of the cellular diffusion, the development of liver fibrosis/-cirrhosis can be safely monitored. We suggest further research to investigate changes in microperfusion and cellular diffusion longitudinally, and want to highlight that, with progressive liver disease being apparently inherent to the Fontan circulation, steps have to be taken concerning potential treatment options for liver disease in Fontan patients. Therefore, future studies should focus on reversibility of this liver disease, and the effects and timing of potential treatment options, including heart transplantation, Fontan conversion or a late Fontan takedown.

Appendix 1. The Fontan operation

The Fontan operation is currently the treatment-of-choice for patients who are born with a univentricular heart which is not suitable for a biventricular repair[11,12]. With the Fontan operation, the right atrium or both caval veins are surgically connected to the pulmonary artery, thereby bypassing the subpulmonary ventricle. This means that the systemic venous return flows passively through the pulmonary vascular bed, without the aid of a pumping ventricle. As a consequence, Fontan patients suffer from chronically elevated systemic venous pressure and decreased cardiac output due to decreased ventricular preload and increased ventricular afterload. Over four decades, the short term survival after the Fontan operation improved significantly[16]. However, patients who underwent a Fontan operation are prone to develop several complications on the long-term. The liver is one of the organs that suffer from the unphysiologic circumstances. Both the increased systemic venous pressure and the decreased cardiac output are thought to be underlying causes of the progressive liver damage in the Fontan circulation. The liver damage in the Fontan circulation was first recognized in a 15-year-old girl with severe systemic hypertension due to a conduit stenosis[29]. Nowadays, more evidence is emerging that liver damage is not restricted to single patients with adverse hemodynamic complications, but is inherently related to the un-physiological circumstances of the Fontan circulation[22]. Liver damage in the Fontan circulation presents with disturbed transaminases, coagulation disorders, and can eventually lead to liver fibrosis-, cirrhosis and even hepatocellular carcinoma[34-36]. Because a liver biopsy (which is considered the golden standard) is hazardous in Fontan patients, the search for alternative measures to assess liver fibrosis and cirrhosis is ongoing.

References

1. Amano Y, Kumazaki T, Ishihara M. Single-shot diffusion-weighted echo-planar imaging of normal and cirrhotic livers using a phased-array multicoil. *Acta Radiol* 1998;39(4):440-442.
2. Kele PG, van der Jagt EJ. Diffusion weighted imaging in the liver. *World J Gastroenterol* 2010;16(13):1567-1576.
3. Bakan AA, Inci E, Bakan S, Gokturk S, Cimilli T. Utility of diffusion-weighted imaging in the evaluation of liver fibrosis. *Eur Radiol* 2012;22(3):682-687.
4. Luciani A, Vignaud A, Cavet M, et al. Liver cirrhosis: intravoxel incoherent motion MR imaging--pilot study *Radiology* 2008;249(3):891-899.
5. Patel J, Sigmund EE, Rusinek H, Oei M, Babb JS, Taouli B. Diagnosis of cirrhosis with intravoxel incoherent motion diffusion MRI and dynamic contrast-enhanced MRI alone and in combination: preliminary experience *J Magn Reson Imaging* 2010;31(3):589-600.
6. Lewin M, Poujol-Robert A, Boelle PY, et al. Diffusion-weighted magnetic resonance imaging for the assessment of fibrosis in chronic hepatitis C. *Hepatology* 2007;46(3):658-665.
7. Wang Y, Ganger DR, Levitsky J, et al. Assessment of chronic hepatitis and fibrosis: comparison of MR elastography and diffusion-weighted imaging. *AJR Am J Roentgenol* 2011;196(3):553-561.
8. Taouli B, Tolia AJ, Losada M, et al. Diffusion-weighted MRI for quantification of liver fibrosis: preliminary experience. *AJR Am J Roentgenol* 2007;189(4):799-806.
9. Namimoto T, Yamashita Y, Sumi S, Tang Y, Takahashi M. Focal liver masses: characterization with diffusion-weighted echo-planar MR imaging. *Radiology* 1997;204(3):739-744.
10. Le Bihan D, Breton E, Lallemand D, Aubin ML, Vignaud J, Laval-Jeantet M. Separation of diffusion and perfusion in intravoxel incoherent motion MR imaging *Radiology* 1988;168(2):497-505.
11. Fontan F, Baudet E. Surgical repair of tricuspid atresia. *Thorax* 1971;26(3):240-248.
12. Kreutzer G, Galindez E, Bono H, De Palma C, Laura JP. An operation for the correction of tricuspid atresia. *J Thorac Cardiovasc Surg* 1973;66(4):613-621.
13. Fredenburg TB, Johnson TR, Cohen MD. The Fontan procedure: anatomy, complications, and manifestations of failure. *Radiographics* 2011;31(2):453-463.
14. Rychik J, Veldtman G, Rand E, et al. The precarious state of the liver after a Fontan operation: summary of a multidisciplinary symposium. *Pediatr Cardiol* 2012;33(7):1001-1012.
15. Hoffman JI, Kaplan S. The incidence of congenital heart disease. *J Am Coll Cardiol* 2002;39(12):1890-1900.
16. Wolff D, van Melle JP, Ebels T, Hillege H, van Slooten YJ, Berger RM. Trends in mortality (1975-2011) after one- and two-stage Fontan surgery, including bidirectional Glenn through Fontan completion. *Eur J Cardiothorac Surg* 2014;45(4):602-609.
17. Greenway SC, Crossland DS, Hudson M, et al. Fontan-associated liver disease: Implications for heart transplantation. *J Heart Lung Transplant* 2015;doi10.1016j.healun.2015.10.015 [Epub ahead of print]
18. Pundi K, Pundi KN, Kamath PS, et al. Liver Disease in Patients After the Fontan Operation. Am J Cardiol 2015; doi: 10.1016/j.amjcard.2015.11.014 [Epub ahead of print]
19. Ozkurt H, Keskiner F, Karatag O, Alkim C, Erturk SM, Basak M. Diffusion Weighted MRI for Hepatic Fibrosis: Impact of b-Value. *Iran J Radiol* 2014;11(1):e3555.
20. Sandrasegaran K, Akisik FM, Lin C, et al. Value of diffusion-weighted MRI for assessing liver fibrosis and cirrhosis. *AJR Am J Roentgenol* 2009;193(6):1556-1560.
21. Kiesewetter CH, Sheron N, Vettukattill JJ, et al. Hepatic changes in the failing Fontan circulation. *Heart* 2007;93(5):579-584.

22. Wolff D, van Melle JP, Dijkstra H, et al. The Fontan circulation and the liver: A magnetic resonance diffusion-weighted imaging study. *Int J Cardiol* 2016;202:595-600.
23. Dijkstra H, Baron P, Kappert P, Oudkerk M, Sijens PE. Effects of microperfusion in hepatic diffusion weighted imaging. *Eur Radiol* 2012;22(4):891-899.
24. Couinaud C. Le foie: etudes anatomiques et chirurgicales. Paris: Masson, 1957;
25. Bismuth H. Surgical anatomy and anatomical surgery of the liver. *World J Surg* 1982;6(1):3-9.
26. Le Bihan D, Turner R, Moonen CT, Pekar J. Imaging of diffusion and microcirculation with gradient sensitization: design, strategy, and significance *J Magn Reson Imaging* 1991;1(1):7-28.
27. Muller MF, Prasad P, Siewert B, Nissenbaum MA, Raptopoulos V, Edelman RR. Abdominal diffusion mapping with use of a whole-body echo-planar system *Radiology* 1994;190(2):475-478.
28. Turner R, Le Bihan D, Maier J, Vavrek R, Hedges LK, Pekar J. Echo-planar imaging of intravoxel incoherent motion *Radiology* 1990;177(2):407-414.
29. Lemmer JH, Coran AG, Behrendt DM, Heidelberger KP, Stern AM. Liver fibrosis (cardiac cirrhosis) five years after modified Fontan operation for tricuspid atresia. *J Thorac Cardiovasc Surg* 1983;86(5):757-760.
30. Safran AP, Schaffner F. Chronic passive congestion of the liver in man. Electron microscopic study of cell atrophy and intralobular fibrosis. *Am J Pathol* 1967;50(3):447-463.
31. Ghaferi AA, Hutchins GM. Progression of liver pathology in patients undergoing the Fontan procedure: Chronic passive congestion, cardiac cirrhosis, hepatic adenoma, and hepatocellular carcinoma. *J Thorac Cardiovasc Surg* 2005;129(6):1348-1352.
32. Kanda T, Yoshikawa T, Ohno Y, et al. Perfusion measurement of the whole upper abdomen of patients with and without liver diseases: initial experience with 320-detector row CT. *Eur J Radiol* 2012;81(10):2470-2475.
33. Wang X, Xue HD, Jin ZY, et al. Quantitative hepatic CT perfusion measurement: comparison of Couinaud's hepatic segments with dual-source 128-slice CT. *Eur J Radiol* 2013;82(2):220-226.
34. Johnson JA, Cetta F, Graham RP, et al. Identifying predictors of hepatic disease in patients after the Fontan operation: a postmortem analysis. *J Thorac Cardiovasc Surg* 2013;146(1):140-145.
35. Asrani SK, Asrani NS, Freese DK, et al. Congenital heart disease and the liver. *Hepatology* 2012;56(3):1160-1169.
36. Asrani SK, Warnes CA, Kamath PS. Hepatocellular carcinoma after the Fontan procedure. *N Engl J Med* 2013;368(18):1756-1757.